Pyroelectricity of Water Ice

Hanfu Wang,[†] Richard C. Bell,*[,‡] Martin J. Iedema,[†] Gregory K. Schenter,[†] Kai Wu,[§,#] and James P. Cowin*[,†]

Pacific Northwest National Laboratory, Box 999, M/S K8-88, Richland, Washington 99352, Chemistry Department, The Pennsylvania State University, Altoona College, Altoona, Pennsylvania 16601, and Beijing National Lab for Molecular Sciences, College of Chemistry and Molecular Engineering, Peking University, Beijing 100871, China

Received: May 19, 2007; Revised Manuscript Received: February 21, 2008

Water ice usually is thought to have zero pyroelectricity by symmetry. However, biasing it with ions breaks the symmetry because of the induced partial dipole alignment. This unmasks a large pyroelectricity. Ions were soft-landed upon 1 μm films of water ice at temperatures greater than 160 K. When cooled below 140−150 K, the dipole alignment locks in. Work function measurements of these films then show high and reversible pyroelectric activity from 30 to 150 K. For an initial ∼10 V induced by the deposited ions at 160 K, the observed bias below 150 K varies approximately as 10 V × $(T/150\ \mathrm{K})^2$. This implies that water has pyroelectric coefficients as large as that of many commercial pyroelectrics, such as lead zirconate titanate (PZT). The pyroelectricity of water ice, not previously reported, is in reasonable agreement with that predicted using harmonic analysis of a model system of SPC ice. The pyroelectricity is observed in crystalline and compact amorphous ice, deuterated or not. This implies that for water ice between 0 and 150 K (such as astrophysical ices), temperature changes can induce strong electric fields (∼10 MV/m) that can influence their chemistry, ion trajectories, or binding.

Introduction

Water ice is normally considered to have zero pyroelectric or piezoelectric properties.[1] A material has nonzero piezoelectricity if when compressed or extended (strained) in one direction, it reversibly develops (or changes pre-existing) voltage differences between one or more of its opposite sides. Quartz is a good example of such a material. Similarly, if it develops a voltage across opposing sides upon heating, it is pyroelectric. Since temperature and strain are symmetric to spatial inversion, while the generated voltages are antisymmetric, it is necessary that the material must not be symmetric with respect to inversion if it is to have nonzero pyro-/piezoelectricity properties. It also may need to lack certain other symmetries such as *S*-type reflection/rotation symmetries, some of which can also depend on the internal symmetries of the unit cell. For these reasons, ice Ih (hexagonal lattice) and ice Ic (face-centered cubic ice) are normally thought to have zero pyro-/piezoelectricity. However, this is only true if the dipoles of the water molecules have no net orientation. As shown in Figure 1, left, water ice can, in principle, be configured so that each water molecule contributes a full 0.57 of each molecule's dipole magnitude to the overall *z*-axis (vertical) dipole. Such a fully oriented water ice should have very large pyro-/piezoelectric response.

However, fully ordered versions of pure ice I are not easy to come by (see also KOH-doped ices below).[2–4] "Normal" ice I has no net dipole orientation and thus is more like that shown on the right side of Figure 1. Accordingly, the pyro-/piezoelectric properties of water ice have been almost always assumed to be zero, and the very few values (other than zero) that have, to our knowledge, been reported in the literature were dismissed as likely unreliable.[1]

It is easy to create slightly proton ordered ices, and these should possess nonzero pyro-/piezoelectricity. The common misconception is that these would have very small to negligible pyroelectricity. Commercial pyroelectrics such as PZT are only slightly aligned as well. Partial alignment of water ice can be done by cooling ice down below 150 K while under a strong external electric field (see page 123 in ref 2). The frozen polarization still exists even when the external field is removed (creating an electret), or one can add ions to the surface, as shown on the right side of Figure 1, and simply permit the system to dielectrically respond. Most biasing or ion-dosing approaches only achieve on the order of 1% alignment. Yet, this is quite enough to make it strongly pyroelectric.

As shown below, if one polarizes an ice film by precharging it with ions at a temperature where its dielectric constant is large (>150 K) to generate, for example, 10 V of bias across it, the pyroelectric effects seen when the temperature is dropped to 50 K are on the order of 100% of this starting voltage. This is a very large change and means that any experiment measuring or sensitive to the electric potential on ice may be strongly be affected by this phenomenon. Where cold ices abound, as in the Oort cloud of our solar system, this may influence transport of ionic species and facilitate reactions. It may play a role in helping cement icy grains together to make planetesimals form rapidly in planetary nebula, as discussed in an earlier paper of ours.[5] In ref 6, we briefly reported some information about this pyroelectric phenomenon, though with largely incorrect hypotheses to explain it.

The electrical and polarization properties of water ice, with or without added ions, are remarkably rich throughout the temperature range of 0−200 K. Some of these properties have

* To whom correspondence should be addressed. E-mail: jp.cowin@pnl.gov (J.P.C.); rcb155@psu.edu (R.C.B.).
[†] Pacific Northwest National Laboratory.
[‡] The Pennsylvania State University.
[§] Peking University.
[#] E-mail: kaiwu@chem.pku.edu.cn.

10.1021/jp073870c CCC: $40.75
Published on Web 04/22/2008

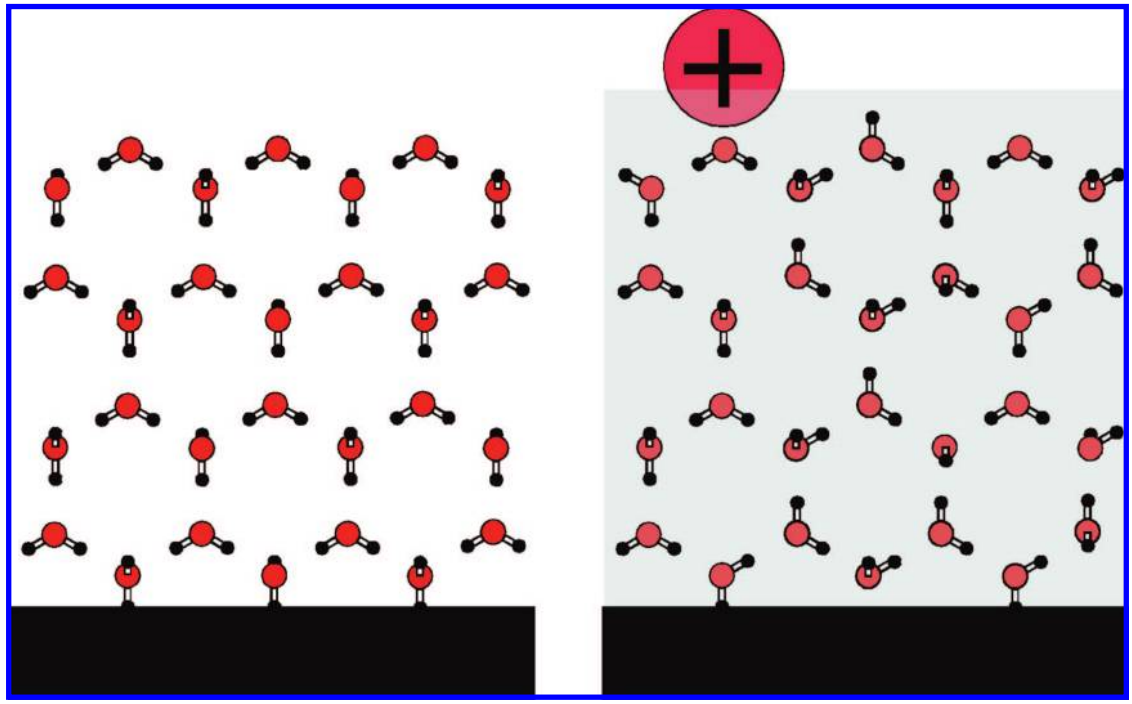

Figure 1. Left: 2-D schematic of a fully proton ordered ice on a metallic substrate with a large net dipole (the maximum possible). Right: The same with no net dipole. The shading on the right is the dielectric "filler" in the VSM ice "model" used later in the paper.

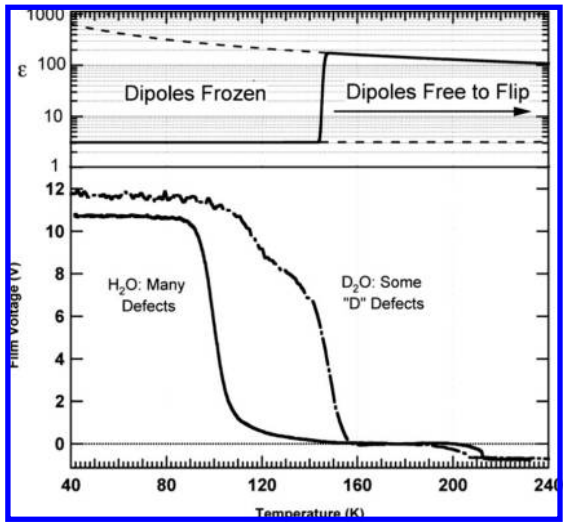

Figure 2. Top: Dielectric behavior versus T for defect-free D_2O ice (solid line). Bottom: Crystalline ice films charged with ions at $<<100$ K, where $\varepsilon \approx 3$. Then, the T is slowly ramped upward while the film voltage is monitored. Left: H_2O, 2620 ML, grown at 170 K. Right: D_2O, 2880 ML, grown at 150 K. The sudden decreases near 100–120 K (solid curve) and between 120 and 150 K (dashed curve) are due to the dielectric constant greatly increasing. The H_2O film was dosed with Cs^+, and the D_2O was dosed with D_3O^+.

been well-known for many years,[2,4] and some large effects are only recently being understood.[3,7–9] It is important to understand some of the general properties of water ice and water ice films in this temperature regime. Bulk liquid water or water ice both have similarly large dielectric constants above 150 K ($\varepsilon \approx 180$ at 150 K[2]), as shown in Figure 2. This is dominated by the ability of water molecules in ice to flip their orientation in response to an external electric field, so as to lower the overall energy (and the net electric field). Small amounts of thermally generated mobile L and D hydrogen bonding defects[2] facilitate this, all the while preserving the net number of hydrogen bonds. This is termed the high-temperature dielectric constant ε_{HT}. The kinetics of reorientation of waters becomes progressively slower as the temperature drops, becoming longer than many seconds at a temperature that depends both on whether it is deuterated ice or not and on its precise thermal history. This temperature ranges from 100 to 150 K, depending on the isotope and number of defects in the ice. The range of temperatures has to do with how many "L" or "D" defects preexist[2,4] and probably more subtle things, like how they might be bound to each other and with what orientation they are bound with respect to the crystal lattice. The mobility of these defects seems to be the catalyst for flipping water molecule orientations, and 124 K or lower has been reported for mobility of some of the defects. [7] The transition from having dipoles that can flip to having dipoles that are kinetically unable to flip can occur over just a few degrees. Therefore, one can (roughly) characterize this as occurring at a specific temperature, which we will call the "cessation temperature" for a particular ice film, T_c. Below this temperature, the water molecules no longer can reorient on the seconds to hour time frame of these experiments, and the effective dielectric constant falls to around 3.[2,4,7] This ε_{mw} (mw here indicates microwave frequency, at which many conveniently measure it) is caused by the electronic polarizability of water molecules, plus field-induced bond bending, stretching, and twisting of water dipoles.

Water ice normally has no net water molecule orientation. There is considerable debate about whether there is a proton-ordered, lowest energy state of water. Pure water ice shows no indication of this, though inhomogeneously doped water ice (from freezing KOH solutions) shows some subtle changes in the electrical properties from 72 to 150 K that might indicate some orientation transition might occur near 15 K. KOH-doped ices do show some sort of phase transition at 72 K, which has been attributed to a proton ordering leading to "ice XI".[2] However again, pure ice shows no such effects. Water ice, when grown from the vapor onto single-crystal Pt(111) substrates, forms basal-plane-aligned ice, which is quite smooth, stable, and crystalline when the temperature at which the ice is vapor

deposited (T_{growth}) is between 140 and 220 K with coverages larger than 50 monolayers (ML).[10] For $T_{growth} < 120$ K, water ice grows amorphously; and as T_{growth} drops, it can become increasingly "fluffy" (for background gas or large-angle directed dosing)[11] on a molecular scale and shows fragile metastabilities.[5,12] When $T_{growth} < 120$ K, brief annealing to around 120 K creates stable and compact amorphous ice. If annealed to around 155 K, it converts to compact polycrystalline ice. The dielectric properties of compact amorphous ice are similar to those of crystalline ice (with the high dielectric constant persisting to about 20 K lower temperatures[3]). When ice is vapor-grown, a very slight and metastable alignment (sometimes termed ferroelectricity) of the water dipoles can occur[3] in the bulk due to the asymmetry of the growing ice−vacuum interface. This can create very large net voltage differences between the base and top of the growing ice films, on the order of –0.02 V for each monolayer of growth. This decreases rapidly as T_{growth} increases, becoming very tiny by 155 K and disappearing for T_{growth} above this temperature. This slight alignment is sometimes observable in the experiments reported here, though it disappears upon annealing to or slightly above 155 K.

Very recently, for thick films of water ice grown upon Pt(111), we observed dissociation of water at the Pt−ice interface and subsequent hydronium segregation at the vacuum−ice interface[8,9] for T_{growth} between 153 and 190 K. This created water films with a natural positive film voltage. This effect could be blocked by surface oxygen (and enhanced by surface hydrogen). In some cases in this experiment (done before those of refs 8 and 9), the films were grown under conditions where this dissociation/segregation could be and was occasionally seen to occur. In the data presented here (taken <1 year earlier), such spontaneous positive film voltages were not seen and may have been blocked by persistent Pt surface oxygen from water impurities or the more frequent and aggressive high-temperature oxygen treatments performed on the Pt to reduce contaminates in these experiments compared to those in refs 8 and 9. The pyroelectric effects discussed in this paper were consistently evident in both the earlier and more recent studies. Further, these pyroelectric effects are independent of surface pretreatments (such as oxygen or hydrogen) or the presence of intervening complete monolayers of hydrocarbons on the Pt surface. It is a true bulk effect in the ice.

Experimental Section

All experiments have been conducted in an ultrahigh vacuum chamber with a base pressure of 2×10^{-10} Torr. The chamber was fitted with a molecular beam doser, low-energy ion source, mass spectrometer, Auger spectrometer, and Kelvin probe. A 1 cm diameter Pt(111) single crystal was used as a substrate for film deposition. It was cleaned routinely by ion sputtering and oxygen exposure (to remove carbon), and the cleanliness was checked by the Auger spectrometer. The substrate can be heated radiatively by filaments mounted behind it and cooled by a helium closed cycle refrigerator. The D_2O and H_2O used in the experiments were degassed by freeze–pump–thaw procedures at least three times.

Crystalline ice films were deposited between 155 and 170 K via a tube doser. When needed, amorphous ice films were grown at $T < 120$ K. The tube doser consists of a small baffled chamber with an opening of 1 cm placed about 1 mm away from the substrate. This should have given a uniformity of dosing of around 5%. This was verified by the zero-order thermal desorption spectra, obtained at close to constant temperature. A low-energy and pure (ions/neutrals >100) ion beam source provided Cs^+ and D_3O^+ ions. This was used to bias the ice films so as to obtain a partial dipole alignment. The ion beam was used to "soft land"[6,13,14] ions at typically 0.5−1 eV energy, low enough to not chemically damage the ions nor the ice films. The heat of condensation (~0.4 eV) plus the impact energy (~0.5 eV) could, in principle, melt a region containing about 15 water molecules, but this localized heating would only persist for picoseconds before vibrational energy diffusion cooled it, limiting the possible effects and transport. It has been shown that neither Cs^+ nor hydronium ions move through the water ice films for $T < 190$ K .[7] All of the pyroelectric results presented here were identical whether Cs^+ and D_3O^+ ions were used. The ions are not bulk dopants and create their effect on the bulk ice only by their long-range collective electric potentials. Thus, there is no reason to expect the pyro-/piezoelectric effects in the water ice polarized by their presence on the ice surface to be in any way sensitive to the identity of the ion used. This is consistent with the fact that no difference is seen whether Cs^+ or hydronium ions are used.

The ions on top of the ice films create a net electric field across the film, as given by the standard capacitor eq 1

$$V_{film} = \frac{Q \cdot L}{A \cdot \varepsilon(T) \cdot \varepsilon_0} \quad (1)$$

where the amount of ions deposited is Q, the film thickness is L, the film area is A, the dielectric constant of water is ε, and ε_0 is the vacuum permittivity. The film voltage V_{film} for the ice film was determined with a Kelvin probe. The Kelvin probe directly measures the contact potential difference (CPD) between the sample and the gold-coated Kelvin probe tip (i.e., CPD = $\Phi_{Probe} - \Phi_{Sample}$, where Φ_{Probe} and Φ_{Sample} are the work functions for the probe and the sample, respectively). Our V_{film} is basically equal to the CPD minus any contribution due to purely interfacial work function changes. The CPD value of the clean Pt crystal using our probe is around –0.6 V, which is almost independent of temperature. The measured CPD values for ice films include an about +0.5 V contribution from the water-induced work function changes localized at the Pt−ice interface. This disappears when the multilayer water desorbs by 200 K. Since in this study we are interested in V_{film}, we offset the measured Kelvin probe signals to eliminate this nearly constant shift. This causes the reported V_{film}'s to drop to around –0.5 V at or above 200 K. The voltage developed after ion deposition is independent to whether Cs^+ or hydronium ions are used for a given deposited charge. The multistep ion deposition,[6,13,14] whereby the ions are permitted to charge up the surface until most of the ions are reflected, the sample is biased 0.5−1 V more negative, more ions are added, and the process is repeated until the desired charging is obtained, gives very uniform charging with little damage but makes it difficult to measure the net deposited ions to better than 50%. The ion doses are more accurately determined from eq 1, the observed film voltage, and the known dielectric constants. The doses range from about 20 to 3000 nC/cm^2 or about 0.0001 to 0.018 ions per every water molecule in the topmost water layer.

The Kelvin probe signals were often measured while the temperature was raised or lowered. At the same time, the mass spectrometer signal could be monitored. When little water desorption was expected, the mass spectrometer filament was turned off to prevent spurious charging of the ice film by stray electrons (pA). When the temperature was ramped from 150 to 200 K (typically at 0.1 K/s), the mass spectrometer signal provided a temperature-programmed desorption (TPD) spectra. The temperature of the multilayer desorption peak of the water

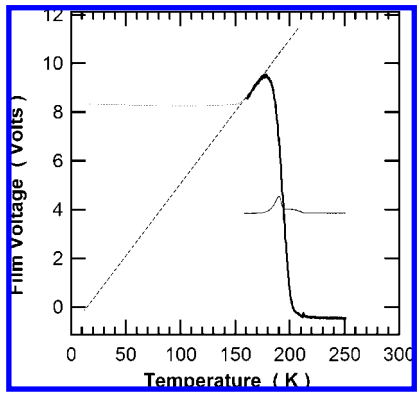

Figure 3. The "expected" film voltage and a portion of the data. A crystalline 5000 ML D_2O ice film was grown at 155 K and subsequently ion dosed (Cs^+) at 160 K. After temperature cycling this film five times between 50 and 150 K, the temperature was then slowly raised from 50 K at 0.2 K/s while the film voltage was monitored. The experimental voltage (solid line) is shown for $T > 160$ K. The water desorption trace is also displayed as a thin-line curve centered near 200 K. The dashed and dotted lines show two variations of the "expected" behavior (see text) in the 50−160 K region.

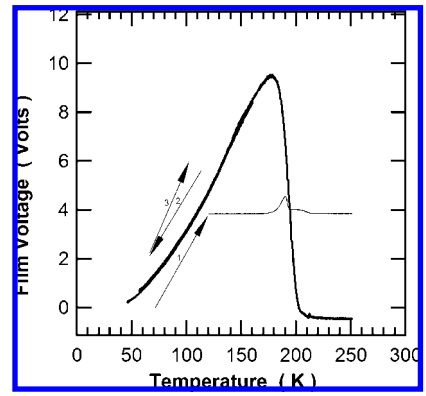

Figure 4. Reversible film voltage change of crystalline D_2O ice with Cs^+ ions dosed at 160 K. The film is the same as that shown in Figure 3. However, now, the 50–160 K part of the actual data curve is also shown. Note that it differs drastically from either "expected" behavior shown in Figure 3 (see text).

was used to determine the initial coverage of the ice films,[3] with each nominal "monolayer" of water being 3.6 Å thick.

Results and Discussion

Basic Observational Phenomena. Figure 2 shows data for crystalline H_2O and D_2O ice films, grown at 170 and 150 K, respectively, which span the widest range of activation temperatures that we have observed for the high dielectric constant behavior (100 and 150 K, respectively). After growth, they were cooled to between 30 and 40 K and dosed with Cs^+ and D_3O^+ ions, respectively, to charge them to about 11–12 V. From the charge needed to reach this voltage, ~20 nC, one can estimate that the ice dielectric constant was near 3 (as expected). Then, the films were warmed at a constant rate. The D_2O film is more typical of the other data presented in this paper, and the major drop in voltage near 150 K is as expected for the large dielectric constant change (to about 180) near that temperature. The H_2O film growth conditions used to produce the data shown in Figure 2 seems to have produced many internal ice defects, which permit the dielectric constant to become active even near 100 K, instead of the expected 140 K. The partial drop in voltage for the D_2O curve near 125 K is specific to using hydronium ions and is related to the D defects that they produce under some conditions.[7]

In Figure 3, we show data where the ion dosing is done at a higher temperature, where the dielectric constant should be much higher. Proportionally more ions were used so as to make the film voltage readily observable. We prepared a crystalline D_2O ice film by vapor deposition at 155 K followed by Cs^+ ion dosing at 160 K. After this the sample was cooled to about 50 K, it was then warmed up to 160 K at 1 K/s followed by cooling down again to around 50 K. This heating/cooling cycle was repeated five times before taking the data shown in Figure 3. The sample was then ramped at 0.2 K/s while CPD and TPD were recorded at the same time. Figure 3 shows the data for $T > 160$ K as T increased smoothly until the water ice film desorbed. The film voltage drops rapidly as the film desorbs near 200 K (the TPD waveform is double-peaked due to the partial obscurance of the desorption by the Kelvin probe). From 160 to about 180 K, the film voltage rises nearly linearly with temperature.

This is just as expected (dashed line) for a dielectric constant varying inversely proportionally to temperature (normal for ice), and thus, the voltage is linear (via eq 1). If the temperature were to be dropped well below 160 K, the film voltage cannot follow the dashed curve indefinitely. At lower than around 150 K for the D_2O ice film, we should expect that water molecules will no longer be able to change their alignment as the temperature is further dropped. What is expected to happen then, according to our original thinking and that of several (informally polled) water ice experts, is that the film voltage would simply stop changing and would follow the dotted curve at low temperature. This guess we term "*V*-naive".

Figure 4 shows what really happens. The data is from the same experiment as that shown in Figure 3, except that now the film voltage during the last portion of the five heating/cooling cycles between 50 and 160 K is also shown. The film voltage continues to change rapidly with temperature, all the way down to 50 K and to within a percent or two, completely reversibly. The first part of the heating/cooling cycles (not shown) was similar to the traces shown. In other runs, this reversible voltage change was found to continue down to 30 K. The "reversible" voltage region shows little or no hysteresis for temperature drops/rises from 0.1 to 1 K/s. When such a ramp is interrupted, the voltage stays very constant fairly indefinitely (>1 h).

An early and incorrect hypothesis that was considered was that, for some reason, the dielectric constant was staying active all the way down to 30 K. The functional form of the observed film voltages was often very accurately fit by $V_{film} \approx a \times T^2$, with small offsets along either axis (for $30 < T < 120$ K). This would be compatible with $\varepsilon(T) = b/T^2$ in eq 1. However, while $\varepsilon(T) \propto 1/T$ is a natural behavior for a dielectric, $\varepsilon(T) \propto 1/T^2$ is not. Materials approaching their ferroelectric transition from either above or below (where the transition is driven by the alignment energy itself) will have $\varepsilon(T) \propto 1/|T - T_0|$, where T_0 is the ferroelectric transition temperature.[15] However, there seemed to be no precedent for it to be proportional to $1/T^2$. Also, no known mechanism exists that would permit dipole flipping in water ice down to 30 K.

Another experiment was done to directly show that the effects seen in Figure 4 were not due to the dielectric coefficient being active down to 30−50 K. A film was made similar to the one used in Figure 4 but with the two ion doses, one done at 160 K and the second done at 50 K. With only the first ion dose added (at 160 K) so as to charge it to about 3.8 V, this film showed a "reversible" voltage change like that seen in Figure 4. Then,

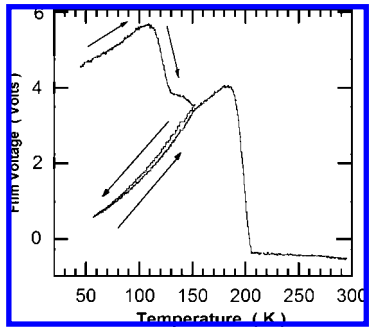

Figure 5. The dielectric constant is shown to be low (≈3) for 50 < T < 110 K by adding new ions to previously dosed water ice. A 2000 ML ice film was grown at 160 K. Then, a first group of ions were dosed at 165 K to make a system that behaved much like that seen in Figure 4. Next, the sample was cooled to 60K, and a small amount of additional ions were added. Then the sample was ramped in T upward from 60 K. The film voltage drop between 110 and 150 K is where the dielectric constant activates. Then, when T was dropped and then reramped, the data resembles that of Figure 4. This shows that the dielectric constant is small (~3) near 60 K, not large (>200).

the second ion dose was added on top of the film at 50 K. If the dielectric constant was still active at 50 K, it would need to be on the order of 600, and this would be immediately obvious from the small change in the voltage per unit charge added. This was found not to be the case. The second dose of ions caused the film voltage to change rapidly. Only about 1/60 of the ion dose used for the first group of ions was able to raise the film voltage from about 0.5 (at 50 K) to about 4.5 V. This showed that the ions in the second dose were sensing a dielectric constant with a value near 3. Next, upon warming, this doubly dosed system showed behavior that further confirmed that the dielectric constant is inactive in this low-temperature regime. Figure 5 shows the film voltage measured for the doubly dosed film as the temperature was slowly raised, starting from 40 K. The film voltage rose from an initial 4.5 V to a maximum near 110 K and then dropped rapidly. This rapid drop is similar to that seen in Figure 2 for ions dosed at low temperature on water ice. This corresponds to the second group of ions finally sensing a large dielectric constant for T > 110 K. This is irreversible. The temperature ramp was then stopped at 150 K, and the sample was allowed to cool back down to 55 K. Figure 5 shows that the second group of ions now appears to behave no differently than those deposited earlier at 160 K. This made it clear that low-temperature behavior shown in Figure 4 was not due to some mysteriously active (down to 30 K) dielectric constant.

To further disprove that the effect has anything to do with the mobility of defects or hydroniums keeping the dielectric constant active to 30 K, we examined amorphous ice. Figure 6 shows a 1000 ML H_2O film, grown amorphous and "fluffy" at 32 K and then compacted without crystallization at 130 K.[11] When dosed with ions at 130 K, where its dielectric constant is active, the films upon subsequent cooling showed results that were very similar to that for crystalline ice. Therefore, the effect does not require an ordered crystal lattice.

Figure 6 shows data comparing H_2O and D_2O films. A H_2O film was grown at similar conditions as those for the D_2O film seen in Figure 4 and is shown with the last portion of the Figure 4 data. The H_2O data is offset by about 7 K to a lower temperature than that of the D_2O data. This is fairly typical of the isotope effects seen for a variety of kinetics for surface-bound water or ice films. Figure 6 also shows a hybrid fit to the data using a line above the apparent T_c and a quadratic below T_c. The fit is nearly within the line width of the plot.

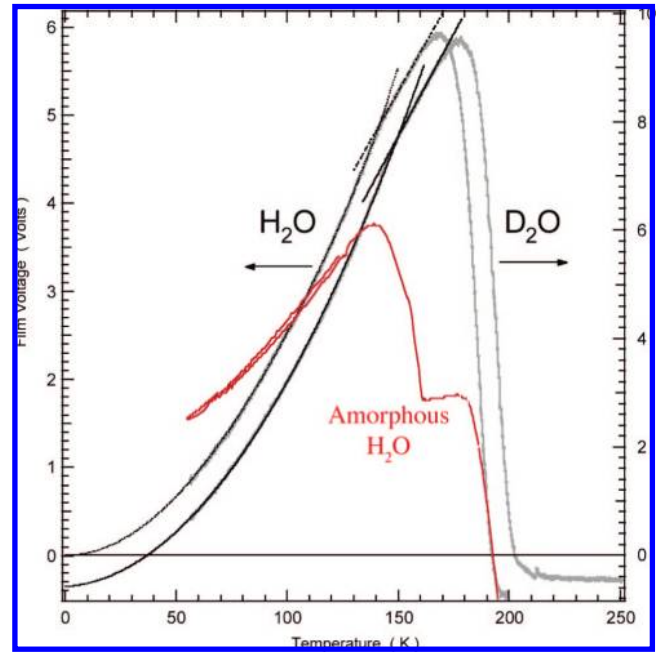

Figure 6. Shown is an amorphous 1000 ML water film (in red), grown at 32 K, annealed at 130K, and ion-dosed with D_3O^+ at 130 K. Also shown is the difference between H_2O and D_2O crystalline ice. Right: 5000 ML D_2O ice as in Figure 4. Left: Crystalline H_2O ice (7500 ML) dosed with Cs^+ ions (grown at 155 K, ion dosed at 160 K, the latter heated to 160 K at 1 K/s and cooled to ~50 K for five cycles before this measurement). Curve fits shown are quadratic on the left portion of each curve and linear on the right portion, with the switches occurring at ~141 and ~146 K (T_c).

Pyroelectricity as the cause of the observations was not immediately recognized due to a simple yet attractive misconception. Pyroelectricity is due to thermally induced changes in unit cell dimensions, bond angles, or similar properties. In general, for 100 K temperature changes, one would (correctly) expect these quantities to change by perhaps 1%. Thus, one might (incorrectly) expect that would alter a 10 V film voltage by around 1%, not by 100% as observed. However, numerical comparisons of the results seen for the ice to those for well-known pyroelectric materials support the case that it could be pyroelectricity. Pyroelectricity of a material is usually expressed via some intrinsic parameter, such as the volts per meter created across opposite faces of a slab when the temperature is raised by 1 K. A very commonly used pyroelectric material is lead zirconate titanate (PZT). A particular sample of powdered PZT in a flexible ferroelectric polymer matrix (poled at 2×10^7 V/m) had a pyroelectricity of about 4.7×10^4 V/m/K (at 70 C).[16] A 3000 ML film of water ice in this study is about 1.0×10^{-6} m thick. Therefore, 10 V voltage changes over 100 K would require a specific pyroelectricity of about 1×10^5 V/m/K. This is similar to the PZT. Since this quantity is also (typically) proportional to the poling electric field, a yet-more dimensionless pyroelectric coefficient is calculated by dividing the previous one by the poling voltage. For the PZT composite, this gave 0.0025/K. The 10 V ice film was "poled" at 10 V/1.0×10^{-6} m, yielding a pyroelectric coefficient of 0.01/K, four times that for the PZT composite! It would appear that pyroelectricity could be involved for the water ice.

Just how pyroelectricity for water ice (and for many other substances) can be so large is well-known for polar systems that exhibit large changes in the dielectric constant versus temperature. We illustrate how this happens in some detail by

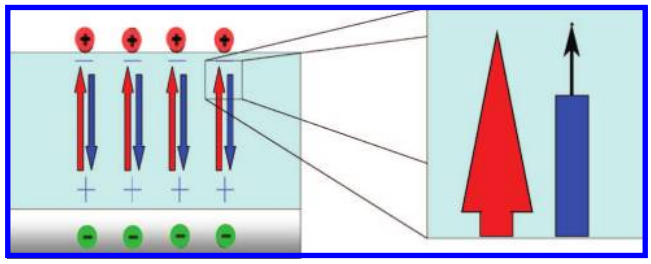

Figure 7. The difference between two large voltages creates the observed voltage. The arrows to the left of the pairs represent the voltage for ions present with the dielectric response without any reoriented waters. The right arrows are the voltages due to the field-aligned dipoles, giving a net voltage (small arrow) that is only a few percent of the big arrows.

comparing our results to a simplified theoretical model system used to analyze the phenomena.

Conceptual Model. We build a conceptually very simple model (VSM) for solid ice: a rigid lattice with no dangling hydrogen bonds, a global space filling polarizability that matches the high frequency dielectric constant $\varepsilon_{mw} \approx 3$, an ability to flip water orientations, and lacking any of those potentials or dynamics that so complicate most models of water. This is shown on the right side of Figure 1. One could carve this solid into identical isolated polar and polarizable gas-phase water molecules and then try to parametrize it to match the properties of gaseous water. Even when one has an excellent knowledge of the polarizability and dipole and multipole fields around an isolated polar molecule (or model molecule), it is very difficult to accurately predict the bulk dielectric constant of a molecular solid made from these molecules,[17] short of using full-scale molecular dynamic or Monte Carlo simulations.[18] This is because (1) the high-temperature dielectric constant ε_{HT} in dense polar solids or liquids is extremely sensitive to the smallest details of the multipolar potentials between different molecules and to T-dependent correlation effects between adjacent dipoles and (2) not quite as obvious, that ε_{mw} is also fairly sensitive to these details. However, predictions are much easier in the other direction; we use the experimentally known ε_{HT} and ε_{mw} versus T to provide what we need to know about the amount of dipole alignment in our ice films and parametrize the VSM to match the solid ice data (not gas phase).

We assume the ball and stick core of each water molecule has a nonpolarizable dipole of strength μ_0 when isolated in the vacuum with no filler. A slab, L thick, of this VSM ice rests on a perfect metal, which exists at $z < 0$. An external field is created by placing point charges on the surface just inside of the dielectric. This polarizes the filler and alters the alignment of water dipoles (at high enough T). A charge $-Q$ will appear at the metal substrate surface from the polarization of the metal. The net voltage across the film is obtained by a double integration of the Poisson equation (the second integration after multiplying by z and integrating by parts), as in eq 2.

$$V_{film} \equiv \langle V(x,y,z=L+\delta)\rangle_{xy} - \langle V(x,y,z=0-\delta)\rangle_{xy} = \frac{QL}{A\varepsilon_0} + \frac{\sum_{i=1}^{N} u_0 \cos(\Theta_i)}{A\varepsilon_0} + \int_{z=0}^{z=L} dz(z \times \rho_{filler}(z)) \quad (2)$$

The last three terms correspond to the three sources, (a) the charges Q and $-Q$, (b) the hard dipoles, and (c) the z-axis polarization of the filler (both as polarized by the external Q and by the internal hard dipoles). $V(x,y,z)$ is the exact potential anywhere in or around the ice. $\langle V(x,y,z)\rangle_{xy}$ is the average over x and y of $V(x,y,z)$ on a plane at z. N is the total number of water molecules in the slab, and $\cos(\Theta_i)$ is the alignment of the ith molecule's dipole with the z axis.

Since the physical model has only linear dielectrics and fixed charges, with no fixed voltage boundary conditions, $V(x,y,z)$ is precisely the sum of $V_Q(x,y,z)$ and $V_{HD}(x,y,z)$, where the first is the solution for just the external charge Q above and below a slab of ε_{mw} filler with no dipoles and the second is the solution for the slightly aligned hard dipoles in the filler without Q. This is true regardless of how the waters became aligned. Equation 2 can thus be re-expressed as in eq 3 for any T

$$V_{film}(T) = \left(\frac{QL}{A\varepsilon_0} + \int_{z=0}^{z=L} dz(z \times \rho^{Q}_{filler}(z))\right) + \left(\frac{\sum_{i=1}^{N} u_0 \cos(\Theta_i)}{A\varepsilon_0} + \int_{z=0}^{z=L} dz(z \times \rho^{HD}_{filler}(z))\right) = \frac{QL}{\varepsilon_{mw}A\varepsilon_0} + \frac{N\langle u_0 \cos(\Theta)\rangle_N}{\varepsilon_{mw}A\varepsilon_0} = \frac{QL(T)}{\varepsilon_{mw}(T)A(T)\varepsilon_0} + \frac{M(T)\langle |u_0 \cos(\Theta)|\rangle_N(T)}{\varepsilon_{mw}(T)A(T)\varepsilon_0} \quad (3)$$

The last part of eq 3 shows all terms that depend on T (even slightly). In real (or VSM) crystalline ice, placed on its basal plane (Ih) or its (111) plane (Ic) the waters have dipole components along the z axis that cluster very closely (exactly) near either $+\mu_0\langle|\cos(\Theta)|\rangle_N$ or $-\mu_0\langle|\cos(\Theta)|\rangle_N$. This permits one to define an integer $M(T)$ as the number of dipole "up" molecules minus those "down".

Equation 3, in its final form, permits a clear conceptual picture of how the voltage would be expected to vary with temperature. At temperatures where the dipoles are free to come into equilibrium with the field, eq 1 is valid. Combined with eq 3, this determines $M(T)\mu_0\langle|\cos(\Theta)|\rangle_N$. If the temperature is continuously dropped, eq 3 remains valid, except that $M(T)$ will (nearly abruptly) cease to change below T_c . Then M remains constant at $\sim M(T_c)$ as the temperature drops further. T_c ranges from 100 to 150 K depending on the film, isotope, and preparation.

The magnitudes of the terms in eq 3 for $\varepsilon_{mw} = 3$, $\varepsilon_{HT}(T_c) = 180$, and $V_{film} = 10$ V are 10 V = (180/3)10 V + (−(180/3)10 V + 10 V) = 600 − 590. The observed 10 V is truly the difference of two large numbers, as represented in Figure 7. When all is at equilibrium, these two large numbers track each other closely, with the ~2% small difference equaling the result in eq 1. At temperatures below T_c, M can no longer change; therefore, the two large terms no longer can track each other. Since the denominators of both terms are the same, small (~1%) changes in their values cause only ~1% changes in V_{film}. This we ignore. The numerators in eq 3 can and will change independently, the first as $L(T)$ and the second due to the T-dependent average molecular orientation $\langle|\mu_0 \cos(\Theta)|\rangle$. For T dropping from T_c to 50 K, one would expect L to slightly decrease in magnitude, which decreases the magnitude of the positive first term. Thermal phonons wiggle the molecules and decrease their average orientation $\langle|\cos(\Theta)|\rangle$. Decreasing T lowers the wiggling, increasing the magnitude of the negative second term. Therefore, one might expect (very roughly), for T dropping from T_c to 50 K, that the 600 V term will decrease about 1% to, say, 594, while the second and negative term will

slightly increase in magnitude to about –596. The sum is now –2 V, down from 10 V, very much the kind of effect reported here!

This simple model shows how very small effects, such as thermal expansion and phonon-induced deorientation of a molecular dipole, can be the source of dramatically large changes in the net voltage for a biased ice film when T drops below T_c. Thus, we should expect to have a very observable pyroelectric voltage below T_c. We next will show more data and extract pyroelectric coefficients for water ice and relate them to some piezoelectric effects. To do this, we rewrite eq 3 one last time in terms of direct observables (ignoring some terms which cannot significantly contribute to the larger changes) as in eq 4

$$V_{\text{film}}(T) \approx V_c\left\{1 + \left[\frac{\varepsilon_{\text{HT}}(T_c)}{\varepsilon_{\text{mw}}(T_c)}\right]\left(\frac{L(T)}{L(T_c)} - \frac{\langle|u_0\cos(\Theta)|\rangle_N(T)}{\langle|u_0\cos(\Theta)|\rangle_N(T_c)}\right)\right\} \quad \text{for } T \le T_c \quad (4)$$

Quantitative Analysis and Modeling. In Figure 3, in the temperature range where the ε_{HT} dielectric constant is active, the voltage changes strongly with temperature because of the rapid $1/T$ change of $\varepsilon_{\text{HT}}(T)$. This kind of $V(T)$ effect is usually excluded from any definition of the pyroelectric coefficient $B(T)$ by making $B(T)$ be the temperature derivative of the charge per unit area that flows through a wire that shorts opposite sides of a 1 unit thick slab. For many materials (and it seems to be true for water ice), the voltages and their temperature derivatives are proportional to the "poling voltage" used to initially bias or treat it. To remove this artifact, it is appropriate to further divide by the charge per unit area deposited during the poling. This transforms eq 4 into eq 5

$$B(T) \equiv \left[\frac{A(T_c)}{Q(T_c)}\right]\frac{\partial}{\partial T}\left(\frac{V_{\text{film}}(T)\varepsilon_0\varepsilon(T)}{L(T)}\right) \approx \frac{\partial}{\partial T}\left(\frac{V_{\text{film}}(T)\varepsilon_{\text{mw}}(T_c)}{V_c\varepsilon_{\text{HT}}(T_c)}\right) = \left(\frac{\partial}{\partial T}\frac{L(T)}{L(T_c)} - \frac{\partial}{\partial T}\frac{\langle|u_0\cos(\Theta)|\rangle_N(T)}{\langle|u_0\cos(\Theta)|\rangle_N(T_c)}\right) \quad (5)$$

In eq 5 (where $V_c = V_{\text{film}}(T_c)$), we have ignored temperature derivatives that are too small to strongly alter the film voltage. The middle expression shows how to use ε_{mw} and ε_{HT} to turn experimental data into $B(T)$, and the last term shows how this can be attributed to the physical phenomena. It might appear that the magnifying term $\varepsilon_{\text{HT}}(T_c)/\varepsilon_{\text{mw}}(T_c)$ in eq 4 has been "lost" in eq 5. However, in converting this $B(T)$ back into the observable voltages, including "poling" the material first, one collectively multiplies $B(T)$ by $\varepsilon_{\text{HT}}(T_c)/\varepsilon_{\text{mw}}(T_c)$. Later in this paper, $B(T)$ is obtained for one D_2O and one H_2O data set. Then, the theory is compared to the experimental V_{film} and B.

Gough has measured ε_{mw} between 2 and 200 K.[19] To a few percent from 50 to 150 K, we can use 3.20 for H_2O. For D_2O, we will use 2.96 measured at 80 K.[2] The high-temperature dielectric constants of ice used here are taken from ref 20: $\varepsilon_{\text{HT}}(T) = \varepsilon_{\text{mw}} + b/(T - T_c)$, where b and T_c are 25400 and 0 K for H_2O and 23600 and 27 K for D_2O.

The data from Figure 6 are used to generate $B(T)$. Figure 8 shows the portion of the D_2O data from Figure 6 where there is negligible desorption of the water. The (nearly) linear part does not have the expected x-axis intercept (27 K). Since part of the film voltage is a somewhat variable work function change at the Pt−ice interface, which we need to remove, the curve can be, and is shown to be, shifted vertically to provide the expected intercept. T_c and the shift ΔV were simultaneously least-squares-optimized by fitting the data below $T_c - 4$ to a fifth-order polynomial. This was extrapolated to higher temperature, and its intercept with the extrapolated linear part occurred at what was defined as T_c. The best fit had $\Delta V = +0.445$ V and $T_c = 146$ K . V_c is the voltage where the two extrapolated curves meet. This V_c is slightly higher than the experimental film voltage ($V_{\text{film}}(T)$) at T_c. The fifth-order polynomial, while more stable for extrapolation than higher powers, had some slight systematic deviations from the data. The experimental data was refit with an 11th-order polynomial (up to $T_c - 4$ K) within a few meV. Then, the derivative of this fitted voltage, as scaled in eq 5, was used to produce the experimental $B(T)$ shown in Figure 9. $B(T)$ for $T > T_c$ is zero.

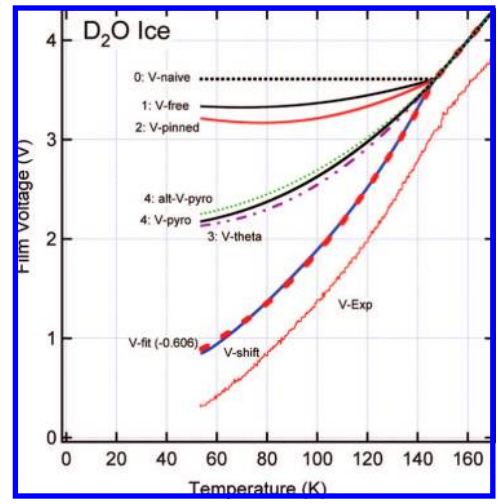

Figure 8. A portion of the D_2O data from Figure 4 (V-Exp). It nearly abruptly changes from linear to curved near 146 K. V-shift is a slightly shifted version of V-Exp (see text) and is shown as an 11th-order polynomial fit to the data, with a break to linear at 146 K. Starting from the naive expectations (V-naive), various contributions to the estimated V_{film} are sequentially added, culminating in V-pyro. V-fit adds one last possible correction (see text).

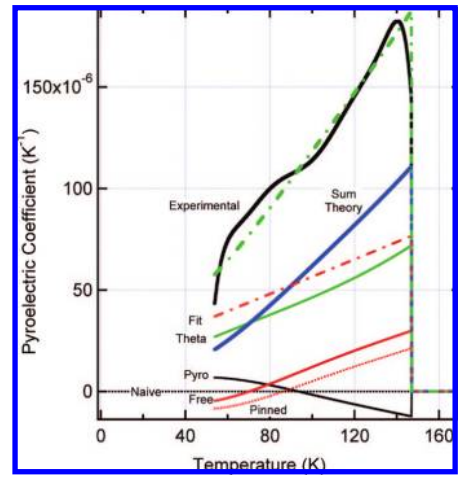

Figure 9. Pyroelectric coefficients for water ice. Experimental is for D_2O data from Figure 2. The Sum Theory curve is the theoretical estimate, and the Pyro, Theta, and so forth terms (explained in the text) are the individual contributions to the total (not cumulative as in Figure 8).

Below begins an attempt to predict the $B(T)$ and $V_{\text{film}}(T)$. The change in L from the thermal expansion was estimated using the experimental linear thermal expansion coefficients for ice[21] and platinum.[12] These were integrated to get the relative sizes of ice and Pt, normalized to 1 at T_c: $S_{\text{ice}}(T)$ and $S_{\text{Pt}}(T)$. $S_{\text{ice}}(T)$ and $S_{\text{Pt}}(T)$ are plotted in Figure 10. The predicted $V_{\text{film}}(T)$ for

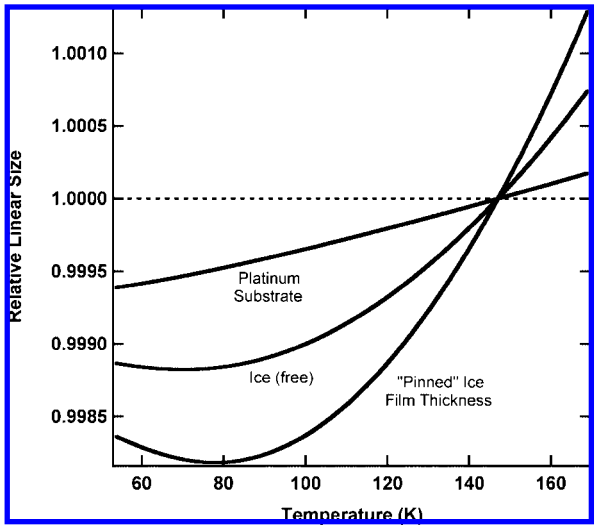

Figure 10. Experimental linear expansion/contraction of the deuterated ice and the Pt substrate. Curves are normalized to unity at 146 K (=T_c). The "pinned" curve shows what happens to the film thickness (in z) when the x and y dimensions of the film are stretched/compressed to match those of the Pt substrate.

changes in L assuming free unconstrained ice is shown in Figure 8 as V-free. This is closer to the experimental data than V-naive.

The ice is assumed to be pinned to the Pt. To prove it is pinned would require lateral measurements of the ice film dimensions or locations of fiducial landmarks, compared to similar ones on the Pt, before and after changing temperatures. Atomic force microscopy might allow such a measurement, but this was not available for this experiment.

If one starts at 150 K with a unit block of free ice that is not pinned to any surface and a unit block of Pt, then at any $T <$ 150, the ice will always be smaller than the Pt. Therefore, upon cooling, the pinned ice experiences a net stretch compared to its free state in the x and y directions to match the Pt. Ice, like most substances, when stretched in one direction, will shrink in other dimensions, in proportion to the Poisson ratio ν. This is taken to be 0.325 here.[2] When stretched simultaneously in x and y by a small fractional amount δ, it is easily shown that the change in the z direction will be $-\nu\delta 2/(1-\nu)$. The change of L via thermal expansion including the effect of pinning is shown in Figure 10, and the resultant voltage is shown in Figure 8 (V-pinned). This moves further toward the experimental curve, though it is still a long ways away.

To furnish estimates for the temperature dependence of the dipole alignment, the ice was modeled with a SPC model. This model has rigid, nonpolarizable water molecules with three fixed point charges of –0.84, +0.42, and +0.42 $|q_e|$, a total dipole moment of 2.27 D, and a 6–12 potential centered on the oxygen.[22] SPC is well-developed and predicts fairly well the structural, dielectric, elastic, thermal expansion, and other properties of real ice and water. One problem is that the experiment will represent an average over many crystallographic variations of slightly polarized water ice. For our primarily qualitative goals, we examined only a particular single ice unit cell of 16 water molecules. We used some experimentally derived numbers to supplement or replace full simulations. A hexagonal ice structure was used, with the basal plane perpendicular to the z direction. The structure of the vapor-grown ice at these temperatures is usually thought to be face-centered cubic,[2] though in both cases, the layer-by-layer structure projected into the z direction is very similar.

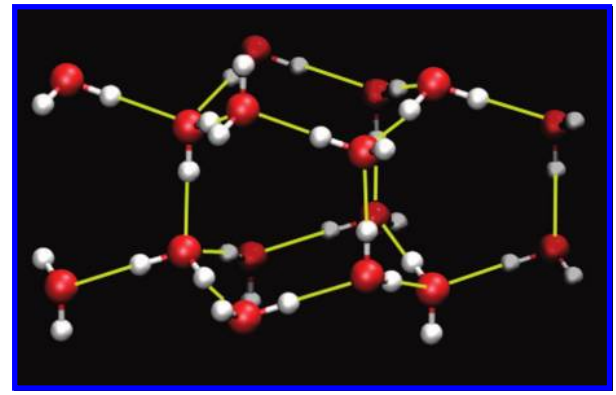

Figure 11. Unit cell of 16 waters for SPC calculation. The z axis (vertical) is a basal plane of this ice Ih.

The 16 molecules were arranged in a unit cell that can fill all of space with no hydrogen bond defects, as shown in Figure 11. A net dipole was created through the particular hydrogen bond arrangement used. Monte Carlo relaxation of the ice (with periodic boundary conditions) was done to eliminate strains and to find the local minimum at a classical 0 K. No waters flipped their orientation during this relaxation. This gave in the z direction (z) a unit cell dipole of –10.26 D, and in x and y, it gave –10.84 and –6.42 D. This is strongly aligned ice, much more so than that in our experiment. In the z direction, there are 4 "up" aligned dipoles and 12 "down" oriented waters ($\sim\pm$1.30 D), as shown in Figure 11.

The energy-relaxed ice has no vibrational motions at all and is the same for either H_2O or D_2O ice. To calculate the effect of vibrations at a temperature T, including the zero-point behavior of this ice, the vibrational normal modes of the unit cell are calculated. For H_2O, these range from 43.4 to 939 cm^{-1}, and for D_2O, they range from 41.4 to 688 cm^{-1} . Their density versus wavenumber matches well with those reported by others[23] (not shown). Since these are rigid molecules, this includes no effects of hydrogen stretches or bends. There are 16 × 6 modes, minus 3 unit cell translational modes (=93). Assuming each mode is harmonically vibrating, with an amplitude taken from a quantized harmonic oscillator and probabilities from a Boltzmann, the time-average effect on the mean alignment of each dipole can be written in terms of the mean square displacement of a harmonic oscillator. The effect on the z component of the dipole, $\langle\cos(\Theta_z)\rangle$ is given in eq 6

$$\frac{\langle\cos(\Theta_z)\rangle(T)}{\langle\cos(\Theta_z)\rangle_0} \approx 1 + \frac{1}{\langle\cos(\Theta_z)\rangle_0}\sum_i\left(\frac{\hbar}{4m_i\omega_i\tanh(\hbar\omega_i/2k_BT)}\right)\times \left(\sum_j \frac{\partial^2\cos(\Theta_{z,j})}{\partial s_i^2}\right) \quad (6)$$

where $\langle\cos(\Theta_z)\rangle_0$ is the zth moment of the dipole with no vibrations and $\langle\cos(\Theta_z)\rangle(0)$ is that at 0 K, including zero point motion. The s_i is the normal mode coordinate of the ith mode, ω_i is its frequency, m_i is the normal mode mass, and j is the sum is over each molecule in the unit cell. This gives $m_0\langle\cos(\Theta_z)\rangle(T)$ as shown in Figure 12. The x and y components (not shown) have a nearly identical relative temperature dependence. The zero-point motion reduces the dipole magnitude in the z direction from 10.266 to 10.046 D for D_2O and to 9.972 D for H_2O.

The 500−700 cm^{-1} normal modes have the largest effect on the dipole alignment, but only through the zero-point vibrations. From 0 to 150 K, these modes show very little change in

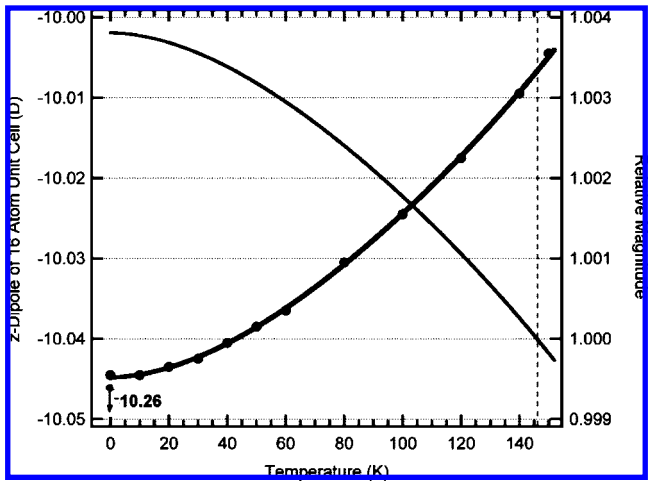

Figure 12. Change in total z-axis dipole component of the 16 water molecule unit cell versus temperature calculated from the SPC model. The line with markers is the absolute dipole, and the other is relative to that at T_c. The single off-scale point shows results at 0 K with no zero-point vibrations.

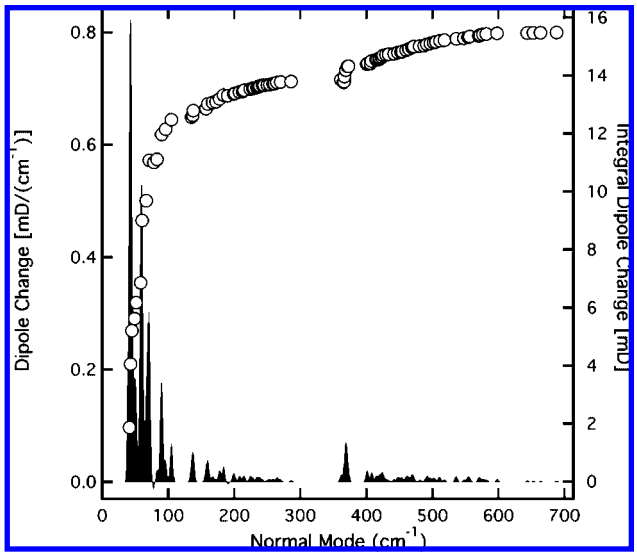

Figure 13. Loss at 150 K of the unit cell's initial z-axis dipole magnitude (|−10.266| D) due to each of the normal mode vibrations (as averaged over a 4 cm^{-1} moving window). This is thermal change beyond that lost from zero-point motion. This is from SPC-simulated D_2O ice. Also shown is the integral (cumulative sum).

amplitude. At 150 K, the loss of dipole alignment beyond that from zero-point motion is shown for each vibrational mode in Figure 13 . It is dominated by <200 cm^{-1} contributions, especially <100 cm^{-1}. At 150 K, the two lowest normal modes (≈2% of the modes) in Figure 12 contribute 26% of the total to the integral, and at 50 K (not shown), they contribute 38%. The full slab with N atoms will have $6N - 3$ vibrational modes, while the unit cell only deals with 93; there are about 3% of the normal modes missing, and they are at low frequency. Therefore, the missing modes could contribute substantially to the decrease in dipole. The loss of alignment reported here is likely a lower limit. This effect versus temperature is added on to that previously discussed and is shown in Figure 8 as "V-theta". This is the largest effect so far and brings the theoretical estimate within about 50% of the experimental.

Next, the piezoelectric voltages are estimated. This simulates the change in average orientation of the dipoles due to thermally induced changes in the size of the ice. This is different than the change in the voltage due simply to the changes in $L(T)/L(T_c)$, which only acts on the ions present. To estimate the pyroelectric terms, the SPC ice unit cell was stretched ±1% in the x, y, and/or the z directions while holding the other dimensions constant. The resulting dipole changes after reoptimizing the six new structures (with no vibrations) are given in Table 1, on the left. The 18 changes can be represented as a tensor e_{ij} acting on the relative strains $\{\Delta x, \Delta y, \Delta z\}$ to within a few to 10% accuracy. The nine elements of this tensor are in the upper right of Table 1. If we assume that the ice film has equal amounts of the structure as that shown in Figure 11 and of the structure after rotating 180° around the z axis, all of the tensor elements except the e_{zz}, e_{zx}, and e_{zy} terms vanish. If we further have equal amounts rotated by ±90°, the e_{zx} and e_{zy} become equal to their average, and then, we can normalize to represent the relative change in the z dipole caused by relative stretching in the z and in the two directions perpendicular to z. These numbers are given in the last row at the right of Table 1. If we choose the x or y direction to be perpendicular to the film face, the second and third rows from the bottom left of Table 1 are the resulting nonzero tensor elements. The ice and our particular choice of unit cell and polarization clearly make for an isotropic material. Nonetheless, the relative axial changes in dipole due to three different on-axis strains (=0.42, 1.02, 0.332) are reasonably similar, more so than the three axial changes due to off-axis strains (−0.32, –0.52, –0.30). The only axis choice of the three that is either truly basal (for hcp ice) or pseudobasal (for fcc ice) is the z axis. This was the choice used.

These piezo-like terms will add to that already predicted. It would be reasonable to apply to the theta term in eq 4 for the strains involved in altering the xy size from that of free ice to that of pinned ice. This is shown in Figure 8 as alt-V-pyro(a). However, the SPC data were used to obtain the purely vibrationally induced theta changes, with the vibrations treated as completely harmonic around the geometry minimum. Therefore, our SPC ice estimate for the theta term has no thermal expansion whatsoever. We applied the experimental expansion coefficient to get the changes in L. However, also needed is the effect of the distortions on the directions of the dipoles that should inherently accompany the free thermal expansion. This is shown as V-pyro in Figure 8. This piezoelectric addition actually moves the theoretical prediction slightly away from the experimental results.

One can sum all of the effects added to V-naive and write eq 7 for D_2O ice

$$V_{\text{theory}}(T) = V_{\text{naive}}(T) + V_c\left(\frac{\varepsilon_{\text{HT}}(T_c)}{\varepsilon_{\text{mw}}(T_c)}\right)\left[1.63\left(S_{\text{ice}}(T) - 1\right) - 0.043(S_{\text{Pt}}(T) - 1) - \frac{\langle\cos(\Theta_z)\rangle(T)}{\langle\cos(\Theta_z)\rangle(T_c)}\right] \qquad \text{for } T \le T_c \quad (7)$$

Figure 9 shows the corresponding estimate of the pyroelectricity coefficient $B(T)$ for D_2O. The comparison of the predicted $B(T)$ and $V_{\text{film}}(T)$ to the experimental is certainly qualitatively encouraging. They have similar shapes. If the theoretical $B(T)$ was multiplied by 1.8, experiment and theory would only be about 10% different. This generality confirms our assignment of these temperature-dependent voltages to the pyroelectric properties of water ice. The SPC prediction being off by nearly a factor of 0.5 from the experiment can be understood via two possibilities.

First is that, here, the harmonic approximation was used to estimate the thermal effects on $\langle\cos(\Theta)\rangle$. In a recent paper,[24] Neumann, using TIP4P water ice, showed that the harmonic

TABLE 1: Change in Dipoles Due to Strain

% stretch			dipole change (original) [D]			tensor elements			
x	*y*	*z*	*x* (−10.8460)	*y* (−6.4204)	*z* (−10.2664)		--*x* [D]	--*y* [D]	--*z* [D]
0	0	0	0	0	0	*x*--	−4.60	1.18	5.70
0	0	−1	−0.0588	−0.0353	0.0352	*y*--	3.30	−6.46	3.41
0	0	1	0.0553	0.0329	−0.0329	*z*--	1.12	5.07	−3.41
−1	−1	−1	−0.0238	−0.0014	−0.0316		relative change (averaged)		
1	1	1	0.0190	0.0004	0.0277	*x*--	0.42	−0.32	−0.32
0	1	0	0.0118	−0.0646	0.0507	*y*--	−0.52	1.01	−0.52
1	0	0	−0.0460	0.0330	0.0112	*z*--	−0.30	−0.30	0.332

approximation when used to estimate the Debye–Waller mean-square displacements was about a factor of 0.8 of the result using a full molecular dynamics treatment of the water ice. If this was also true for the angular displacements in this paper, this would make the theory match the experiment much better. Second, we used SPC and experimental results to insert numbers into our "VSM" model, the latter being used to develop eq 4. Real water is neither SPC ice nor VSM ice. SPC has too small of a ε_{mw} (around 2 instead of about 3[24]). The value of 2 instead of 1 comes from distortions of the lattice in response to external fields. However, it lacks any electronic polarizability (which by itself would give an ε of n^2, or about 1.8). It would be possible to add this to the SPC model just by filling the model with a dielectric of strength ε_f and simultaneously multiplying the SPC charges by ε_f. However, it is easy to show that this would not alter the predicted pyroelectricity of the water ice. Instead, we suggest an improved VSM model (IVSM) that recognizes that externally applied fields will sense a different polarizability than that sensed by an internal dipole. This is entirely due to the detailed relative placement of the dipolar charges and polarizable elements. If one assumes that the external field (as induced by the ions) sees the normally measured $\varepsilon_{mw}(T)$ (there is really no other option here) and that the dipoles see a different locally averaged "dielectric constant" $\varepsilon_{loc}(T)$, one can modify the last line of eq 3 in the denominator of the theta term, replacing $\varepsilon_{mw}(T)$ with $\varepsilon_{loc}(T)$. This notion is reasonable. In our SPC water calculation, for example, despite that it must have an ε_{mw} of about 2 due to field-induced tilting of the dipoles, the average dipole (z direction) of the "up" dipoles in the unit cell is 1.32 D, while the average "down" one is 1.30 D. This is only a 2% difference and shows that the net aligned dipoles here couple only slightly into the librational polarization that accounts for the SPC ε_{mw} being near 2.

One can then calculate that, instead of eq 4, one gets for $T < T_c$ eq 8

$$V_{film}(T) \approx V_c\left\{1+\left[\frac{\varepsilon_{HT}(T_c)}{\varepsilon_{mw}(T_c)}\right]\left(\frac{L(T)}{L(T_c)}-\left\{\frac{\varepsilon_{mw}(T)}{\varepsilon_{mw}(T_c)}-\frac{\varepsilon_{loc}(T)}{\varepsilon_{loc}(T_c)}+\frac{\langle|u_0\cos(\Theta)|\rangle_N(T)}{\langle|u_0\cos(\Theta)|\rangle_N(T_c)}\right\}\right)\right\} \quad (8)$$

If $\varepsilon_{loc}(T)$ was simply half of $\varepsilon_{mw}(T)$, this would have zero effect on V_{film}. However, if they were instead both exactly 3 at T_c but one was +1% larger and the other 1% smaller as the temperature was dropped, this would change the film voltage by a factor of 2 . Just to assess whether eq 8 could plausibly account for the deviation of the theoretical $V_{film}(T)$ (V-pyro in Figure 8) from the experimental, we assumed that this relative difference was equal to $c \times (\varepsilon_{mw}(T) - \varepsilon_{mw}(T_c))/\varepsilon_{mw}(T_c)$ (using $\varepsilon_{mw}(T)$ from ref 19). We found that using $c = -0.606$ gave a very close fit to the experiment (V-fit in Figure 8). One should not overestimate the significance of this particular fit. For example, if in eq 7 one simply replaces 1.63 and –0.043 with best-fit parameters, an even closer fit to the experimental V_{film} results. We also now note that the SPC dipole results inherently included the effects of ε_{loc} at $T = 0$ K. Since this is temperature-independent, any correction of this causes (via eq 8) no changes in the predicted film voltage.

Figure 14 and 15 show the analogous results for H_2O ice. The results are very similar, with rather less effect of the pyroelectric corrections. Other growth conditions for the ices yield similar results, to within 25% of that shown.

Conclusions and Implications

Water ice was found to be strongly pyroelectric once it is "poled", that is, if the dipoles are partially aligned by an external field. This is easily observed as soon as the ice is dropped below

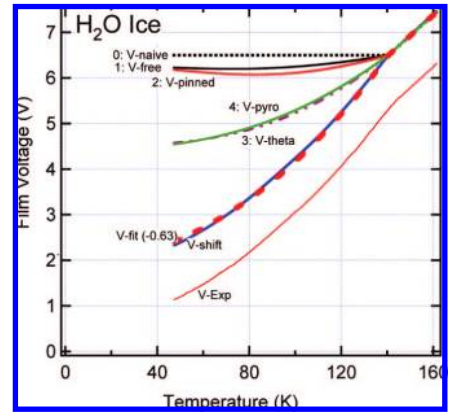

Figure 14. A portion of the H_2O data from Figure 6 (V-Exp), analyzed as described in Figure 8, with $T_c = 141$ K.

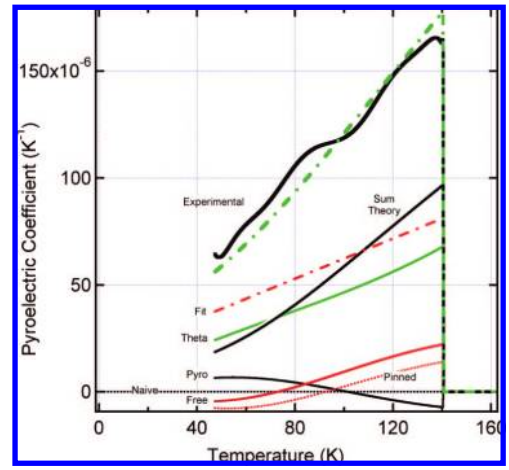

Figure 15. Pyroelectric coefficients for water ice. Experimental is for H_2O data from Figure 6 and is analyzed as described in Figure 9, with $T_c = 141$ K.

the temperature where to dipoles can flip to stay in thermal equilibrium with external fields (<100 to 150 K depending on the ice). The magnitude of this pyroelectricity is in fair agreement with that predicted by the SPC ice model and is similar to that seen for well-known commercial pyroelectric materials. This contradicts assertions of zero pyroelectricity stated in major water ice reviews.[1,2,4] The failure to consistently observe this effect earlier is likely due to the extreme difficulties and ambiguities found when studying macroscopic ice crystals with attached electrodes, which are completely avoided in this study. Any laboratory study that looks at or is sensitive to electric fields of water ice below about 150 K could be strongly altered by this pyroelectricity. Knowing what it is and how to deal with it has been very important for many of this group's soft-landing ion experiments.[3,5,7,8,15] One application of this knowledge to natural situations is in understanding the possible forces between icy grains in presolar nebula.[5] The ability of vapor-deposited ice (even "dirty" mixed ice) to spontaneously partially orient (<2%)[3] during growth anywhere below 150 K or so and create a dipolar voltage difference of thousands of volts had, for some time, suggested to us that this might play some role in icy grains in space. These might make for large external dipole fields that could help ice grains (or ice-coated grains) stick to each other. However, a uniform spherical ice grain would have no net external dipole. For ice grains that had grown while rotating in uniform water vapor, or had unidirectional water dosing, or grew on an asymmetric mineral core, they would be asymmetric, as would ones damaged by collisions. These could have large net dipoles. We calculated how long it would take for the stray charges in space (from photoelectrons, radioactive decay, and cosmic rays) to coat an icy grain possessing a large dipole so as to neutralize the external dipolar field; we found days to weeks.[5] Therefore, it seemed that such dipoles, if present on icy grains in space, would be unlikely to be important as the grains live for millions of years and more. However, it was the understanding of the pyroelectricity of low-temperature water ice that showed that any time such grains warmed or cooled or suffered impacts, the concealed multipolar field would become unmasked. Thus, this might play a very critical role in promoting icy grain adhesion, permitting planetesimals to form.

Acknowledgment. This research was supported by a DOE/BES Chemical Sciences grant and DOE/OBER. The research used the Environmental Molecular Sciences Laboratory, a national user facility sponsored by the Department of Energy's Office of Biological and Environmental Research. We especially thank Professor Athanassios Tsekouras (University of Athens), who first saw this initially puzzling effect in our laboratory.

References and Notes

(1) Fletcher, N. H. *Rep. Prog. Phys.* **1971**, *34*, 913.
(2) Petrenko, V. F., Whitworth, R. W. *Physics of Ice*; Oxford University Press: Oxford, U.K., 1999.
(3) Iedema, M. J.; Dresser, M. J.; Doering, D. L.; Rowland, J. B.; Hess, W. P.; Tsekouras, A. A.; Cowin, J. P. *J. Phys. Chem. B* **1998**, *102*, 9203.
(4) Hobbs, P. V., *Ice Physics*; Clarendon Press: Oxford, U.K., 1974.
(5) Wang, H.-F.; Bell, R. C.; Iedema, M. J.; Tsekouras, A. A.; Cowin, J. P. *Astrophys. J.* **2005**, *620*, 1027.
(6) Tsekouras, A. A.; Iedema, M. J.; Ellison, G. B.; Cowin, J. P. *Int. J. Mass Spectrom. Ion Processes* **1998**, *174*, 219.
(7) Cowin, J. P.; Tsekouras, A. A.; Iedema, M. J.; Wu, K.; Ellison, G. B. *Nature* **1999**, *398*, 405.
(8) Lilach, Y.; Iedema, M. J.; Cowin, J. P. *Phys. Rev. Lett.* **2006**, *98*, 016105.
(9) Lilach, Y.; Iedema, M. J.; Cowin, J. P. *Surf. Sci.* **2008**, submitted.
(10) Zimbitas, G.; Haq, S.; Hodgson, A. *J. Chem. Phys.* **2005**, *123*, 174701.
(11) Kimmel, G. A.; Dohnalek, Z.; Stevenson, K. P.; Smith, R. S.; Kay, B. D. *J. Chem. Phys.* **2001**, *114*, 5295.
(12) Tsekouras, A. A.; Iedema, M. J.; Cowin, J. P. *Phys. Rev. Lett.* **1998**, *80*, 5798.
(13) Strongin, D. R.; Mowlem, J. K; Lynne, K. G.; Kong, Y. *Rev. Sci. Instrum.* **1992**, *63*, 175.
(14) Miller, S. A.; Luo, H.; Pachuta, S. J.; Cooks, R. G. *Science* **1997**, *275*, 1447.
(15) Strukov, B. A.; Levanyuk, A. P. *Ferroelectric Phenomena in Crystals*; Springer-Verlag: Heidelberg, Germany, 1998.
(16) Malmonge, L. F.; Malmonge, J. A.; Sakamoto, W. K. *Mater. Res.* **2003**, *6*, 469.
(17) Frohlich, H. *Theory of Dielectrics: Dielectric Constant and Dielectric Loss*, 2nd ed.; Clarendon Press: Oxford, U.K., 1958.
(18) Fanourgakis, G. S.; Xantheas, S. S. *J. Phys. Chem. A* **2006**, *110*, 4100.
(19) Gough, S. R. *Can. J. Chem.* **1972**, *50*, 3046.
(20) Johari, G. P.; Jones, S. J. *J. Chem. Phys.* **1975**, *62*, 4213.
(21) Röttger, K.; Endriss, A.; Ihringer, J.; Doyle, S.; Kuhs, W. F. *Acta Crystallogr., Sect. B* **1994**, *50*, 644.
(22) Guillot, B. *J. Mol. Liq.* **2002**, *101*, 219.
(23) Gao, G. T.; Zeng, X. C.; Tanaka, H. *J. Chem. Phys.* **2000**, *112*, 8534.
(24) Neumann, M. *J. Chem. Phys.* **1986**, *85*, 1567.

JP073870C